

Combined analysis for anomalous Higgs-gauge boson couplings in γ -proton collisions at the LHC

S. Taheri Monfared*

*School of Particles and Accelerators, Institute for Research in Fundamental Sciences (IPM),
P.O. Box 19395-5531, Tehran-Iran
Department of Physics, Faculty of Basic Science, Islamic Azad University Central Tehran
Branch (IAUCTB), P.O. Box 14676-86831, Tehran, Iran
E-mail: sara.taheri@ipm.ir*

Sh. Fayazbakhsh

*School of Particles and Accelerators, Institute for Research in Fundamental Sciences (IPM),
P.O. Box 19395-5531, Tehran-Iran
Department of Physics, Faculty of Basic Science, Islamic Azad University Central Tehran
Branch (IAUCTB), P.O. Box 14676-86831, Tehran, Iran
E-mail: shfayazbakhsh@ipm.ir*

M. Mohammadi Najafabadi

*School of Particles and Accelerators, Institute for Research in Fundamental Sciences (IPM),
P.O. Box 19395-5531, Tehran-Iran
E-mail: mojtaba@ipm.ir*

The anomalous $HZ\gamma$ coupling is studied through the process $pp \rightarrow p\gamma p \rightarrow pHX$ at the LHC. Utilizing an effective Lagrangian with dimension six operators, new physics effects beyond the standard model are explored in this paper. The applied model includes all kinds of Higgs boson interactions in both CP-even and CP-odd structures. The accurate constraints on anomalous $HZ\gamma$ couplings are numerically analyzed and the results corresponding to the combination of the efficient Higgs decay channels at three different forward detector acceptance regions are presented. Our numerical results propose that the Higgs photoproduction is a reliable complementary channel to study the anomalous $HZ\gamma$ vertices.

*XXIV International Workshop on Deep-Inelastic Scattering and Related Subjects
11-15 April, 2016
DESY Hamburg, Germany*

*Speaker.

1. Status of the Higgs-Gauge Boson Anomalous Couplings

The standard model (SM) of particle physics is well-tested at low energy experiments. However, to explore the new physics (NP) effects on the observed phenomena which are not predicted by the SM, one has to follow non-SM models from a phenomenological point of view. In a model independent approach, an effective Lagrangian with modified interaction terms is proposed, that includes gauge invariant non-renormalizable effective operators after integrating out heavy degrees of freedom beyond TeV scale. There is no evidence of NP discovered at the LHC run-I, up to now, so the physicists attempt to search for signals of NP at the LHC run-II [1].

Following the discovery of the Higgs boson, the anomalous interactions of this field are also theoretically studied in the literature [2, 3]. In the SM, the estimation of the Higgs boson decay width in the $H \rightarrow Z\gamma$ channel is equal to 6×10^{-6} GeV. This is computed from the Higgs particle coupling to photon and Z boson through the loop contributions of W boson and top quark interactions. However, the observed 95% confidence level (C.L.) decay width for this process is about 10 times more than the predicted value by the SM [4, 5]. This discrepancy is a motivating aspect to explore NP effects through the analysis of stringent constraints on both CP-even and CP-odd anomalous $HZ\gamma$ couplings and their collider implications [6].

In the present paper, we focus on the Higgs production cross section considering the anomalous $HZ\gamma$ vertex in a single diffractive process at the LHC and one of the protons in a pp collision remains intact. The fractional proton energy, ξ , as the detector acceptance region for detecting forward protons, is approximately equal to $\xi = E_\gamma/E_p$ where, E_γ and E_p are the energies of the emitted photon and the incoming proton, respectively. In what follows, the constraints on the anomalous $HZ\gamma$ couplings, at center of mass energy $\sqrt{s} = 14$ TeV, are discussed for three different acceptance regions, $0.0015 < \xi < 0.5$, $0.0015 < \xi < 0.15$, and $0.1 < \xi < 0.5$ of the CMS and ATLAS detectors [7].

To generalize the SM with the NP contributions, we start with an effective Lagrangian truncated at dimension six interaction terms, ignoring possible dimension five operators [1],

$$\mathcal{L}_{\text{eff.}} = \mathcal{L}_{\text{SM}} + \sum_i \frac{c_i^{(6)} \mathcal{O}_i^{(6)}}{\Lambda^2} + H.c., \quad (1.1)$$

where, $\mathcal{O}_i^{(6)}$ and $c_i^{(6)}$ represent gauge invariant local operators and dimensionless Wilson coefficients, respectively. In the Higgs sector, the effective operators include the anomalous Higgs-gauge boson interactions [3]. Up to the first power of Higgs particle, the effective Lagrangian can be written in terms of the physical fields as $\mathcal{L}_{\text{eff.}}^{(6)} = HZ_\mu T^{\mu\nu} A_\nu + H.c.$, and the $T^{\mu\nu}$ vertex of the $HZ\gamma$ interaction in momentum space is [8, 9]

$$T^{\mu\nu}(k, Q) = \hat{\alpha}(k, Q) Q^2 g^{\mu\nu} + \alpha_1(k, Q) [Q \cdot k g^{\mu\nu} - Q^\mu k^\nu] + \alpha_2(k, Q) \varepsilon^{\mu\nu\rho\sigma} Q_\rho k_\sigma. \quad (1.2)$$

Here, k and Q denote the Z boson and photon momenta and $\varepsilon_{\mu\nu\rho\sigma}$ is a totally antisymmetric tensor with $\varepsilon_{0123} = 1$. Practically, $(\hat{\alpha}, \alpha_1, \alpha_2)$ are dimensionful independent coefficients whose nonzero values are possibly induced by non-SM heavy particles and can change Higgs production cross sections. In the SM the leading order results are $\hat{\alpha}^{\text{SM}} = \alpha_1^{\text{SM}} = \alpha_2^{\text{SM}} = 0$. In this notation, $\hat{\alpha}, \alpha_1$ are the coefficients of the CP-even operators and α_2 is the coupling in the CP-odd interaction term.

These couplings depend on gauge boson masses, the $SU(2)_L$ coupling constant, g , the weak mixing angle, θ_w , and should also be constrained in searching for NP effects [10].

The Feynman diagram of the Higgs production subprocess $\gamma q \rightarrow \gamma Z q \rightarrow Hq$ at leading order, is illustrated in Fig. 1. In the forward collisions, the emitted photons are commonly considered

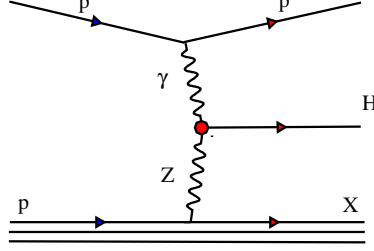


Figure 1: The Feynman diagram of the subprocess $\gamma q \rightarrow \gamma Z q \rightarrow Hq$ at leading order.

massless particles in the equivalent photon approximation (EPA) method [11]. In the EPA the photon spectrum is given by

$$f(E_\gamma, Q^2) = \frac{dN}{dE_\gamma dQ^2} = \frac{\alpha_e}{\pi} \frac{1}{E_\gamma Q^2} \left[\left(1 - \frac{E_\gamma}{E_p}\right) \left(1 - \frac{Q_{\min}^2}{Q^2}\right) F_E + \frac{E_\gamma^2}{2E_p^2} F_M \right], \quad \alpha_e = \frac{e^2}{4\pi}, \quad (1.3)$$

where, F_M and F_E are proton magnetic and electric form factors, respectively [12],

$$F_E = \frac{4m_p^2 G_E^2 + Q^2 G_M^2}{4m_p^2 + Q^2}, \quad G_E^2 = \frac{G_M^2}{\mu_p^2} = \left(1 + \frac{Q^2}{Q_0^2}\right)^{-4}, \quad F_M = G_M^2, \quad \mu_p^2 = 7.78, \\ Q_{\min}^2 = \frac{E_\gamma^2 m_p^2}{E_p(E_p - E_\gamma)}, \quad Q_0^2 = 0.71 \text{ GeV}^2, \quad E_\gamma = E_p \xi, \quad m_p = 0.938 \text{ GeV}. \quad (1.4)$$

In the following, due to the $Q^2 = 0$ approximation the $\hat{\alpha}$ coupling disappears in the scattering amplitude relation. For hard scattering matrix elements, we use the CTEQ14 collaboration results in leading order for the parton distribution functions (PDFs) [13]. The uncertainties due to the PDF choice are estimated as 0.022%, 0.019%, and 0.161% for the first, second, and third acceptance regions at $\sqrt{s} = 14$ TeV, respectively [14]. Integrating the product of the subprocess cross section, the photon spectrum from Eq. (1.3), and also a selected PDF set leads to the total cross section in which the integration limits are determined by corresponding conservation laws. Using

$$y_{\min} = \text{Max} \left[\frac{\omega^2}{4E_p x_{\max}}, E_p \xi_{\min} \right], \quad y_{\max} = \text{Min} \left[\frac{\omega^2}{4E_p x_{\min}}, E_p \xi_{\max} \right], \\ \omega_{\min} = \text{Max} \left[2E_p \sqrt{\xi_{\min} x_{\min}}, m_H + m_q \right], \quad \omega_{\max} = 2E_p \sqrt{\xi_{\max} x_{\max}}, \quad (1.5)$$

the total cross section is derived

$$\sigma = \sum_{q=u,d,s,c,b} \int_{\omega_{\min}}^{\omega_{\max}} \frac{\omega}{2E_p y} d\omega \int_{y_{\min}}^{y_{\max}} dy \int_{Q_{1,\min}^2}^{Q_{1,\max}^2} dQ_1^2 f_\gamma(y, Q_1^2) f_q\left(\frac{\omega^2}{4E_p y}, Q_2^2\right) \hat{\sigma}_{Z\gamma \rightarrow H}(Q_1^2, \omega, y). \quad (1.6)$$

Numerical results of relation (1.6) show that there is no considerable difference between the couplings α_1 and α_2 . In this paper, the factorization scale, μ_f , the renormalization scale, μ_r , and the threshold production scale, Q_2 , are all considered equal to the Higgs mass, $m_H = 125$ GeV.

2. Constraints on the Higgs-Gauge Boson Anomalous Couplings

To perform the numerical analysis on the couplings constraints from the process $pp \rightarrow p\gamma p \rightarrow pHX$ at the LHC, we need the expected background and signal events in the relevant Higgs decay channels. The combined results of three channels $H \rightarrow \gamma\gamma$, $H \rightarrow W^+W^-$, and $H \rightarrow ZZ$ are discussed and the SM branching ratios for these decay channels are 2.28×10^{-3} , 2.15×10^{-1} , and 2.64×10^{-2} , respectively [15]. The number of signal events for each final state, N_{signal} , at a specific integrated luminosity, \mathcal{L}_{int} , is theoretically given by

$$N_{\text{signal}}(\alpha_1, \alpha_2) = \sigma(pp \rightarrow pHX) \times Br(H \rightarrow FF) \times Br(F \rightarrow f_1 f_2 \dots) \times \mathcal{L}_{\text{int}}. \quad (2.1)$$

Here, $F = \gamma, W^\pm, Z$, and $f = l^\pm, \nu_l$ (for $F = W, Z$), also $Br(W \rightarrow f_1 f_2 \dots) = 0.05$, and $Br(Z \rightarrow f_1 f_2 \dots) = 0.12$. We take into account the irreducible background, $(\gamma + q \rightarrow H + q)$, in diffractive processes as well as the reducible ones. As we found, the contribution of the reducible photoproduction processes is rejected by applying the cuts and is more smaller than that of the irreducible process. The background cross sections, calculated with CompHEP v4.5.2 package are in Ref. [16]. The final state includes an intact proton in addition to $\gamma\gamma + jet$, $l_1^\pm l_2^\mp \nu_{l_1} \nu_{l_2} + jets$, and $l_1^\pm l_1^\mp l_2^\pm l_2^\mp$, for $\gamma\gamma$, W^+W^- , and ZZ decay channels, respectively. This state is considered to calculate the background subprocesses. In this analysis, we use the survival factor, $\varepsilon = 0.74$, which depends on the detector performance, and at the scale of Higgs mass results in a $\sim 26\%$ reduction of the expected signal and background cross sections [17]. Moreover, the reconstruction and acceptance efficiencies are not included into the bounds estimations in this paper.

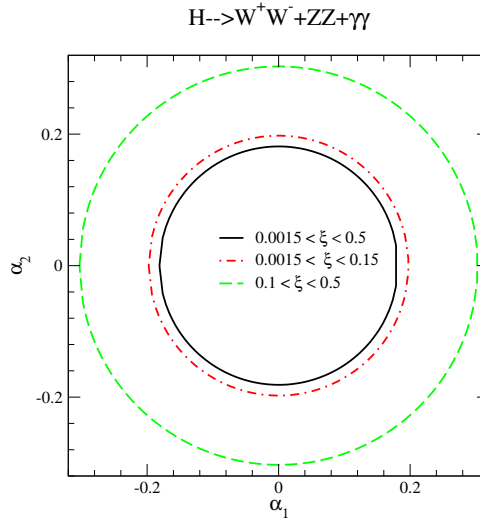


Figure 2: The contour diagrams in $\alpha_2 - \alpha_1$ plane (units in TeV^{-1}) for the combined channel of three different Higgs decay channels with 95% C.L. at $\sqrt{s} = 14$ TeV, $\varepsilon = 0.74$, and for $\mathcal{L}_{\text{int}} = 300 \text{ fb}^{-1}$. The curves are plotted for three different acceptance regions.

The contour diagrams of the bounds in the combined channel are studied in Fig. 2, in $\alpha_2 - \alpha_1$ plane, with 95% C.L. at $\sqrt{s} = 14$ TeV, $\varepsilon = 0.74$, and for $\mathcal{L}_{\text{int}} = 300 \text{ fb}^{-1}$ in three ξ values. As is shown in Fig. 2, the first acceptance region is the most sensitive interval of ξ to the anomalous couplings and this point could be estimated by a counting experiment analysis. Figs. 3 and 4 display the dependencies of $\alpha_{i=1,2}$ to the integrated luminosity and survival factor, respectively. The curves are depicted at $\sqrt{s} = 14$ TeV and for three different acceptance regions. Increasing

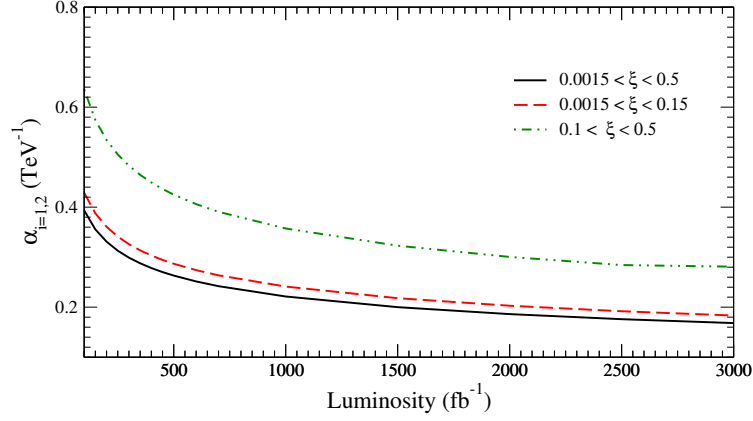


Figure 3: The anomalous couplings as a function of integrated luminosity, at $\sqrt{s} = 14$ TeV and $\varepsilon = 0.74$. The curves are plotted for three different acceptance regions.

the luminosity as well as survival factor provide more restricted bounds in all acceptance regions. To have more realistic constraints, the appropriate cuts, which select the events, are applied on pseudorapidities and transverse momenta of the final state particles. Moreover, some mass cuts to suppress the background events at each decay channel are imposed.

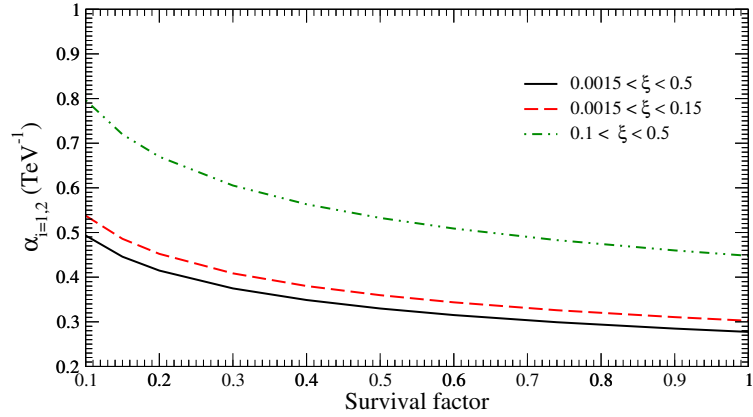


Figure 4: The anomalous couplings as a function of survival factor, at $\sqrt{s} = 14$ TeV and $\mathcal{L}_{\text{int}} = 300 \text{ fb}^{-1}$. The curves are plotted for three different acceptance regions.

The SM loop computation at $m_H = 125$ GeV, ignoring bottom quark contributions, predicts a coupling value of about $\alpha_1 = -4.1 \times 10^{-5} \text{ GeV}^{-1}$ [3]. According to the CMS (ATLAS) measurements at center of mass energy $\sqrt{s} = 8$ TeV and the luminosity $\mathcal{L}_{\text{int}} = 19.6 \text{ fb}^{-1}$, the constraint on the anomalous coupling is $-0.162 \leq \alpha_1 \leq 0.082 \text{ TeV}^{-1}$ ($-0.168 \leq \alpha_1 \leq 0.088 \text{ TeV}^{-1}$) [18]

([19]). Comparing the results of Figs. 2-4 with the corresponding ones reported in Ref. [3], $|\alpha_1| \leq 2 \text{ TeV}^{-1}$, one can find that our proposed channel is more sensitive to probe the $HZ\gamma$ couplings. Following additional processes to suppress backgrounds with a real analysis on experimental data can help to improve the constraints that phenomenologically extracted here. In the present paper, we can emphasize that detecting particles in the forward regions is a reasonable method to explore the anomalous $HZ\gamma$ vertices. We conclude that besides the other channels, the studied Higgs photo-production process is complementary to search for the NP effects at the LHC future run.

ACKNOWLEDGMENTS

This work was supported in parts by Islamic Azad University Central Tehran Branch. I would also like to thank the organizers of DIS2016 for their warm hospitality and financial support.

References

- [1] H. Belusca-Maito, arXiv:1507.05657 [hep-ph].
- [2] A. Falkowski, arXiv:1505.00046 [hep-ph]. C. Englert, R. Kogler, H. Schulz and M. Spannowsky, arXiv:1511.05170 [hep-ph]. T. Han, Y. P. Kuang and B. Zhang, Phys. Rev. D **73**, 055010 (2006) [hep-ph/0512193].
- [3] E. Masso and V. Sanz, Phys. Rev. D **87**, no. 3, 033001 (2013) [arXiv:1211.1320 [hep-ph]].
- [4] S. Chatrchyan *et al.* [CMS Collaboration], Phys. Lett. B **726** (2013) 587 [arXiv:1307.5515 [hep-ex]].
- [5] G. Aad *et al.* [ATLAS Collaboration], Phys. Lett. B **732**, 8 (2014) [arXiv:1402.3051 [hep-ex]].
- [6] T. Corbett, O. J. P. Eboli, J. Gonzalez-Fraile and M. C. Gonzalez-Garcia, Phys. Rev. D **87**, 015022 (2013) [arXiv:1211.4580 [hep-ph]].
- [7] M. G. Albrow *et al.* [FP420 R and D Collaboration], JINST **4**, T10001 (2009) [arXiv:0806.0302 [hep-ex]].
- [8] V. Hankele, G. Klamke, D. Zeppenfeld and T. Figy, Phys. Rev. D **74**, 095001 (2006) [hep-ph/0609075].
- [9] K. Hagiwara, S. Ishihara, R. Szalapski and D. Zeppenfeld, Phys. Rev. D **48**, 2182 (1993).
- [10] P. Achard *et al.* [L3 Collaboration], Phys. Lett. B **589**, 89 (2004) [hep-ex/0403037].
- [11] G. Baur, K. Hencken, D. Trautmann, S. Sadovsky and Y. Kharlov, colliders,” Phys. Rept. **364**, 359 (2002) [hep-ph/0112211].
- [12] V. M. Budnev, I. F. Ginzburg, G. V. Meledin and V. G. Serbo, Phys. Rept. **15**, 181 (1975).
- [13] S. Dulat *et al.*, Phys. Rev. D **93**, no. 3, 033006 (2016) [arXiv:1506.07443 [hep-ph]].
- [14] J. Butterworth *et al.*, J. Phys. G **43**, 023001 (2016) [arXiv:1510.03865 [hep-ph]].
- [15] S. Dittmaier *et al.*, arXiv:1201.3084 [hep-ph].
- [16] A. Pukhov *et al.*, hep-ph/9908288.
- [17] L. A. Harland-Lang, V. A. Khoze and M. G. Ryskin, Eur. Phys. J. C **76**, no. 5, 255 (2016) [arXiv:1601.03772 [hep-ph]].
- [18] [CMS Collaboration], arXiv:1307.7135.
- [19] ATLAS Collaboration, ATL-PHYS-PUB-2013-014, <https://cds.cern.ch/record/1611186>, (2013).